RPE | Radiation Physics & Engineering
A Peer-Reviewed Journal
Published by K.N. Toosi University of Technology
http://rpe.kntu.ac.ir
Research Article

Radiation Physics and Engineering 2025; 6(4):39–45

Design and construction of a quality control phantom for evaluation of the clinical imaging performance of electronic portal imaging devices

Nahid Hajiloo[a,*], Mostafa Mohammadi[b], Farzaneh Ghasemifard[c], Mahmoud Reza Aghamiri[c]

[a] *Radiation Application Research School, Nuclear Science and Technology Research Institute, P.O. Box 31485-498, Karaj, Iran*
[b] *Secondary Standard Dosimetry Laboratory (SSDL), Pars Isotope Co., Karaj, Iran*
[c] *Medical Radiation Engineering, Shahid Beheshti University, Tehran, Iran*

HIGHLIGHTS

- A phantom was designed and constructed for the purpose of quality control of the EPID performance.
- A software was developed to analyze the acquired images, and parameters of image quality.
- Image quality parameters were evaluated using constructed phantom.

ABSTRACT

This study presents the design and construction of a quality control phantom for evaluating the clinical imaging performance of electronic portal imaging devices (EPIDs) used in radiation therapy. The phantom, incorporating lead sheets of varying thicknesses and a plexiglass scaling component, enables the assessment of key image quality parameters, including Noise, Uniformity, Contrast-to-Noise Ratio (CNR), Signal-to-Noise Ratio (SNR), Contrast, and pixel-to-millimeter scaling. A dedicated software application, developed using LabVIEW, facilitates automated and standardized analysis of EPID images. The phantom was tested across two radiotherapy centers, revealing differences in EPID performance, with Center A demonstrating lower Noise (0.5 vs. 1.6), better Uniformity (1.9 vs. 9.3), and higher CNR (69.3 vs. 45.6) and SNR values compared to Center B. The phantom's design, inspired by established models like the Las Vegas and PTW phantoms, supports both qualitative and quantitative evaluations, meeting TG142 standards for spatial resolution (>2 mm). This work highlights the efficacy of tailored quality assurance tools in enhancing EPID performance, ensuring precise radiation therapy delivery and improved patient outcomes.

KEYWORDS

EPID QC phantom
Image quality parameters
Radiotherapy
Verification

HISTORY

Received: 7 June 2025
Revised: 25 August 2025
Accepted: 29 August 2025
Published: Autumn 2025

1 Introduction

The application of ionizing radiation, is utilized in radiotherapy to effectively eradicate or diminish cancerous tissues. This treatment approach is considered one of the key methods in cancer treatment, along with surgery and chemotherapy. The utilization of this approach either independently or in conjunction with additional therapeutic interventions has resulted in the recovery of around 40% of individuals diagnosed with cancer. The objective of radiotherapy is to expose cancerous tissue to a high dose of radiation while safeguarding the adjacent healthy tissue, resulting in minimal treatment-related complications. Due to the difference in sensitivity between healthy tissue and cancerous tissue, treatment is performed selectively, resulting in an increase in the dose effects on the tumor and a reduction in the side effects on healthy tissue. Therefore, treatment in each session must be completely reproducible in terms of the level of conformity of the distribution of the delivered dose to the target tissue and the estimated dose of the treatment planning system (Peca et al., 2017; Noble et al., 2024; Kry et al., 2017; Lee et al., 2016; Diklic et al., 2013; Huang et al., 2017). The outcome of radiation treatments is dependent on the received dose to the volume of the target and the healthy surrounding tissues. The correlation between radiation dose and biological impacts on different types of tissues is characterized through dose-response curves. Based on these curves, an increase in dose will result in an improvement in localized tumor control. On the other hand, the steep slope of these curves indicates that a small deviation in the dose transfer rate will result in significant changes in tumor

*Corresponding author: nhajiloo@aeoi.org.ir

https://doi.org/10.22034/rpe.2025.528889.1279

control probability and healthy tissue complications (Diklic et al., 2013; Huang et al., 2017; Cremers et al., 2004; El-Bassiouni et al., 2006). This demonstrates the importance of precision and quoracy in the dose delivery and the essential requirement of verifying the therapeutic dosimetry. The required accuracy for dose delivery in radiation therapies is reported to be ±5% according to the dose-response curves (El-Bassiouni et al., 2006; Gagel et al., 2002; Kruse et al., 2002). The possibility of ensuring such accuracy in the delivery of tissue absorption dose can be realized only by verifying the treatment and identifying sources of uncertainties for each patient.

The initial aim of design and introducing electronic imaging portal systems in the treatment room was to assess the patient's geometric position and decrease treatment uncertainties. These systems have effectively taken the place of the multi-stage film imaging procedures. The process of taking images using film is laborious and time-consuming, therefore it is typically carried out on a weekly basis. In contrast, the EDID has the capability to capture images during each session, and even multiple images within a single treatment session. The digital nature of these images also allows for quantitative assessments and analysis of results, facilitating the identification and rectification of uncertainty sources in real-time during treatment (Gagel et al., 2002; Kruse et al., 2002; Tzomakas et al., 2023; McGarry et al., 2007). An additional application of these increasingly prevalent systems is portal dosimetry based on imaging during treatment.

Modern linear accelerators are equipped with advanced EPID designs that utilize amorphous silicon technology, resulting in superior image quality compared to older devices that rely on film-based imaging or ionization chambers. Currently, the application of EPID in radiation therapy has become an essential component, providing digital images that can enhance visualization and interpretation. The confirmation of the image is dependent on the precision of the acquired data and is partially influenced by the algorithms used in the post-processing phase. Modern radiation therapy has evolved to become image-based, expanding the role of the EPID in patient setup and portal verification to encompass broader applications such as MLC QA, localization of implantable markers in IGRT, IMRT QA, and absolute dosimetry (McGarry et al., 2007; Association et al., 2004; Boudet et al., 2022; Li et al., 2017). Every vendor offers its unique post-processing software alongside the EPID to assist in the manual or automated visualization of the treatment area. The successful execution of these responsibilities necessitates the establishment of QA protocols. Although the majority of reports emphasize the importance of quality control and the implementation of an internal phantom for personal organizational applications, there is still a significant absence of widespread access and comparative data. A suitable phantom for quality assurance of EPID system is essential; it lack could compromise the accuracy of treatment goals in IGRT or IMRT. Initial approaches to the visual assessment of portal images are primarily qualitative and subjective. However, the precision required in imaging and dosimetry within modern radiation therapy necessitates consistent image quality and quantitative evaluations that are robust, accurate, precise, and automated. Various types of quality control phantoms, such as illustrated in Fig. 1, are available for the quality assessment of amorphous silicon EPIDs (Li et al., 2017; Cho et al., 2015; Herman et al., 2001; Klein et al., 2009a; Dogan et al., 2023).

This study involved the design and construction of a phantom utilizing available materials, aimed at facilitating quality control of the Electronic Portal Imaging Device (EPID) system. Subsequently, the EPID systems of selected radiation therapy centers were evaluated for quality assurance using this phantom. Additionally, as a progression of this research, a software application was developed to analyze EPID images. This application was constructed utilizing the LabVIEW programming language and includes a user interface tailored for the assessment of quality control tests related to EPID.

2 Materials and Methods

2.1 Phantom design and construction

The interaction of radiation is categorized based on the type of interaction and the material with which it occurs. This classification includes elastic and inelastic scattering, or alternatively, interactions can be divided into absorption and scattering. Another perspective categorizes interactions into coherent and incoherent types. Also, photon interactions can be categorized into two main types: absorption and scattering. Absorption includes processes such as the photoelectric effect, pair production, and photon decay. On the other hand, scattering encompasses Compton interactions and Rayleigh scattering, with Compton scattering being a form of inelastic scattering and Rayleigh scattering being elastic in nature. The scattering of the predominant photon interaction at an energy level of 6 MV, occurs during the imaging process of the patient, which necessitates the use of 2 to 5 radiation monitor units. In the quality control of the EPID, we select uniform conditions to assess the imaging status. A phantom, the design stages of which will be detailed below, is constructed to evaluate the physical parameters of the image and is subsequently exposed to radiation.

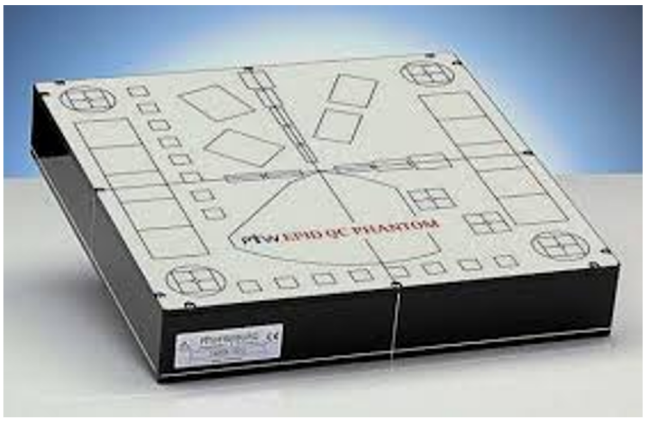

Figure 1: An illustration of the PTW EPID QC phantom.

Lead is a chemical element with the atomic number 82. This heavy metal is characterized by its high density and relatively low melting point compared to most other metals, classifying it as a soft metal. Among stable elements, lead possesses the highest atomic number. It is not only economically viable due to its significant attenuation of high-energy X-rays but also melts at a relatively low temperature of 327 °C, facilitating its use in industrial molding processes.

The phantom incorporates lead sheets that come in three specified thicknesses: 1 mm, 1.5 mm, and 2 mm. These sheets are all crafted from lead with a purity of 99%.

In the design of lead shields, lead sheets of three different thicknesses are arranged in 15 cuts to ensure that they exceed half the thickness of the absorber in response to radiation exposure. For the analysis of low contrast clarity, a thickness that is double that of one-tenth of the absorber was utilized in the construction of the Phantom component. In the production of a series of parallel blades aimed at examining spatial resolution and high contrast resolution, sheets of 99% lead were initially prepared in three different thicknesses. These sheets were then processed through a rolling machine and subsequently measured before being cut using a guillotine and cutter.

In the central section of the Phantom, designed similarly to the Las Vegas Phantom and the PTW Phantom, we conduct a qualitative and visual assessment of the contrast resolution. This contrast differentiation is achieved by creating holes of varying diameters and depths in a lead cube, which is produced through casting in a steel mold. An increased number of holes observed in imaging indicates a superior contrast resolution of the electronic portal imaging system. The criteria for image quality and system performance encompass the following aspects:

2.2 Phantom irradiation

The phantom was irradiated using two different Elekta, linear accelerators at two radiotherapy centers, referred to as Center A and Center B. Irradiation was performed with 6 MV X-ray beams in a controlled setup to ensure consistent imaging conditions. The distance to the phantom surface (SSD) was established at 100 cm, and the radiation field was defined as 15×15 cm^2. The radiation dose for capturing the image was determined to be 2 MU. For Noise and Uniformity measurements, flood field images were acquired without the phantom. For other parameters (CNR, SNR, Contrast, and scaling), the designed phantom was irradiated, and the resulting images were analyzed to evaluate EPID performance.

2.3 Image Quality Factors

The following image quality parameters were assessed using the acquired EPID images:

2.3.1 Noise Sensitivity Index (NSI)

Noise serves as an indicator of the fluctuations in the random signal of the detector. To ensure quality control of the epidemic, an initial image was captured in an open field to assess the level of noise present in the treatment room and any random disturbances from the imaging device. Noise is calculated as the standard deviation of pixel values from the mean in an image. In this work, the noise parameter is defined as the standard deviation of pixel values in a flood field, which can be calculated using the following relationship:

$$Noise = \sigma_{flood} \tag{1}$$

2.3.2 Uniformity

The purpose of this parameter is to ensure that in a flood field, the maximum signal of the pixels does not exceed the minimum signal by a certain specified value. This means that the pixel readings must remain within a defined range.

$$Uniformity = \frac{P_{max} - P_{min}}{P_{max} + P_{min}} \tag{2}$$

2.3.3 Signal to noise ratio (SNR)

The calculation of the Signal-to-Noise Ratio (SNR) was performed using the specified formula:

$$SNR = \frac{\mu_{ROI}}{\sigma} \tag{3}$$

In this context, μ_{ROI} represents the average pixel value within the region of interest, while σ denotes the standard deviation related to that region. The signal-to-noise ratio (SNR) can be utilized to gauge the existence of a signal against a noisy environment, thereby providing a valuable measure for evaluating the quality of images.

2.3.4 Contrast (spatial resolution)

The Contrast parameter is defined based on the darkest and the brightest parts of the image. The objective is to determine the range of the imaging system.

$$Contrast = \mu_{light} - \mu_{dark} \tag{4}$$

2.3.5 Contrast to noise ratio (CNR)

The contrast-to-noise ratio quantifies the capacity for visual detection of an object of a specified size and serves to assess the distinguishability between two regions of interest (ROIs) within an image. This metric provides a valuable estimate of the impact of noise and is computed using the following formula **?**:

$$CNR = \frac{|\mu_{light} - \mu_{dark}|}{\sigma_{dark}} \tag{5}$$

where, μ_{light} is the mean of the pixel values in the "lightest" region, μ_{dark} is mean of the pixel values in the "darkest" region, and σ_{dark} is the standard deviation of the pixel values in the "darkest" region of an image.

Table 1: Results of the image quality factors for two different radiotherapy centers.

Image Quality Factors							
Center	Noise	Uniformity	CNR	SNR		Contrast	Pixel/mm
				SNR-dark	SNR-light		
A	0.5	1.9	69.3	221.0	90.6	39.7	0.2512
B	1.6	9.3	45.6	124.4	80.3	45.5	0.2508

2.3.6 Scaling (pixel per millimeter)

In an image, we are dealing with pixel quantities. To convert pixel values into size and distance parameters, a conversion factor from pixels to millimeters is required. In this study, a phantom made of plexiglass was designed with spherical marble components made of steel. As illustrated below, six points with specified distances have been established within this phantom. These distances were cut using a laser on a sheet of plexiglass. A view of the irradiated image is presented below. Utilizing this image and the software developed for this work, the pixel-to-millimeter parameter value is obtained.

2.4 Software Development

In this study, a program has been developed using LabVIEW programming language to expedite the extraction of quality control parameters for EPID and to standardize the process of extracting these parameters. An overview of this program is illustrated in the Fig. 2. As depicted in the figure, this program consists of six distinct modules named: Noise, Uniformity, CNR & SNR, Long pairs, Spatial resolution, and Pixel per millimeter. Users could input EPID images through a graphical interface, select the desired analysis module, and obtain results for the specified parameters. The software processed flood field and phantom images to compute the image quality factors based on the equations provided, ensuring consistent and reproducible assessments. By inputting an image through the program's input window and selecting the analysis module, the results are displayed.

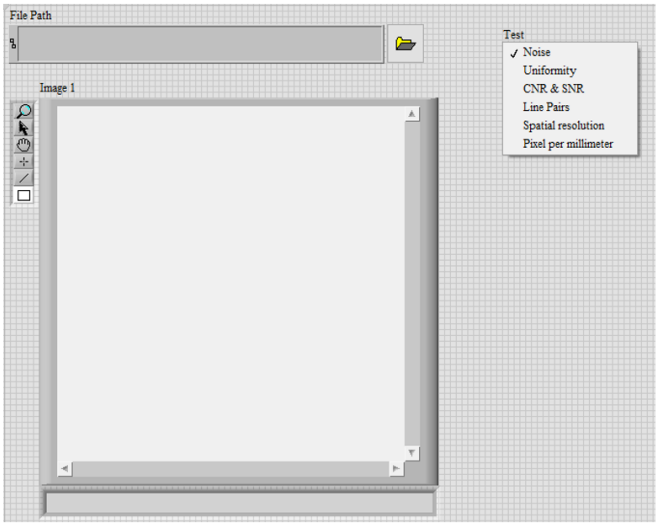

Figure 2: An overview of developed program, for image analyzing.

3 Results and discussion

The quality control phantom, designed and constructed using lead sheets and a plexiglass scaling component, was utilized to evaluate the imaging performance of electronic portal imaging devices (EPIDs) at two radiotherapy centers, referred to as Center A and Center B. A schematic of the designed and constructed phantom is presented in Fig. 3. The phantom was irradiated using 6 MV X-ray beams from linear accelerators, and the resulting images were analyzed using a custom-developed LabVIEW-based software to extract key image quality parameters: Noise, Uniformity, Contrast-to-Noise Ratio (CNR), Signal-to-Noise Ratio (SNR), Contrast, and pixel-to-millimeter scaling. The results for these parameters are summarized in Table 1.

Noise, calculated as the standard deviation of pixel values in a flood field image (Eq. (1)), was 0.5 for Center A and 1.6 for Center B, indicating lower random signal fluctuations in Center As EPID system. Uniformity, determined using Eq. (2), was 1.9 for Center A and 9.3 for Center B, suggesting that Center A's EPID exhibited significantly better pixel signal consistency across a flood field. These measurements were conducted without the phantom, using flood field images to establish baseline performance.

The Contrast-to-Noise Ratio (CNR) and Signal-to-Noise Ratio (SNR) were evaluated using phantom images. CNR, calculated per Eq. (5), was 69.3 for Center A and 45.6 for Center B, reflecting Center A's superior ability to distinguish between regions of interest. SNR, based on Eq. 3, was computed for both dark and light regions. For Center A, SNR values were 221.0 (dark) and 90.6 (light), while for Center B, they were 124.4 (dark) and 80.3 (light), indicating better signal clarity in Center A, particularly in darker regions.

Contrast, assessed as the difference between the mean pixel values of the brightest and darkest regions (Eq. (4)), was 39.7 for Center A and 45.5 for Center B. The spatial resolution module of the software standardized the qualitative assessment by comparing the number of visible holes in the phantom image to the actual number of holes in the lead cube (Fig. 4). Center B demonstrated slightly higher contrast, suggesting better differentiation between bright and dark regions, though both centers met the TG142 (Klein et al., 2009b) standard for spatial resolution (>2 mm).

To obtain the conversion factor from pixels to millimeters, a scaling phantom as illustrated in the Fig. 5 is utilized. The Scaling phantom and its image were used for calibrating distances and thickness in developed softwire. The results of the phantom image analysis using the

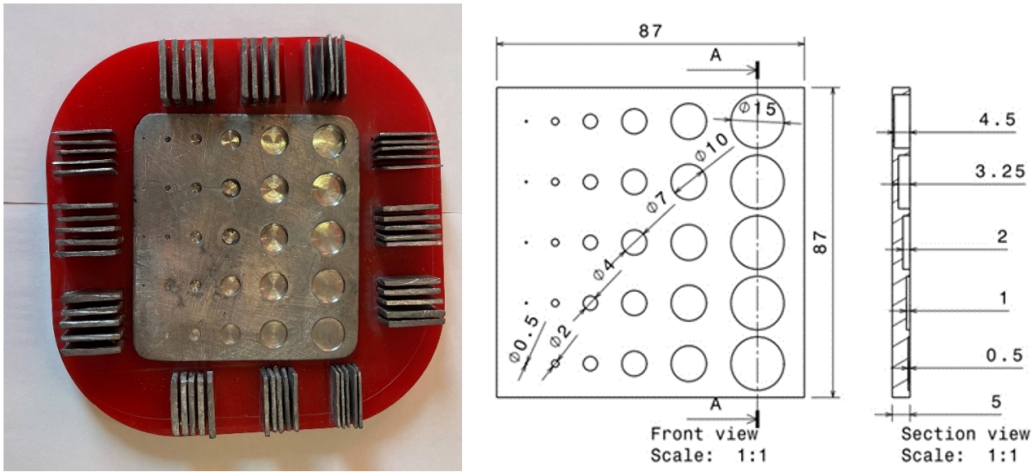

Figure 3: A schematic of the designed and constructed phantom.

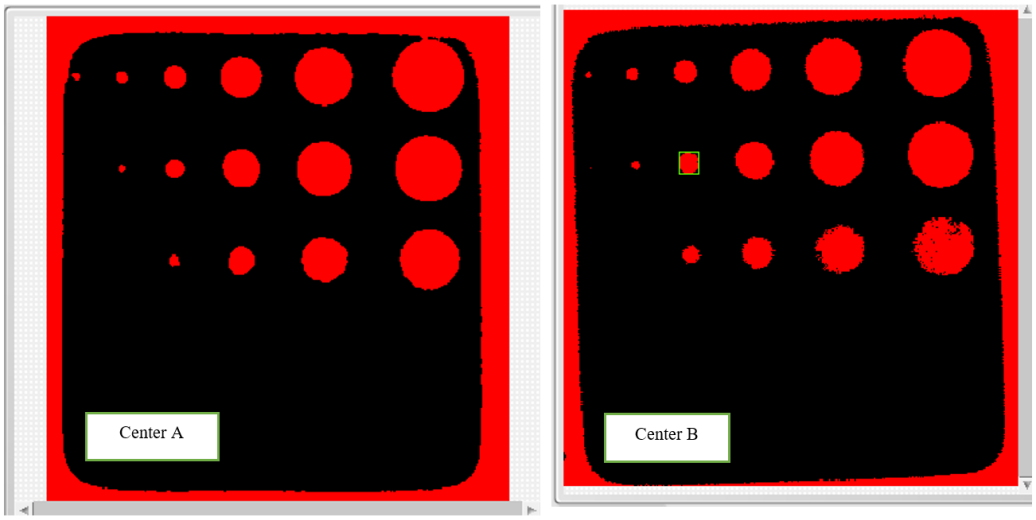

Figure 4: The results of the Spatial resolution (contrast) test analysis for two different devices, developed by the software.

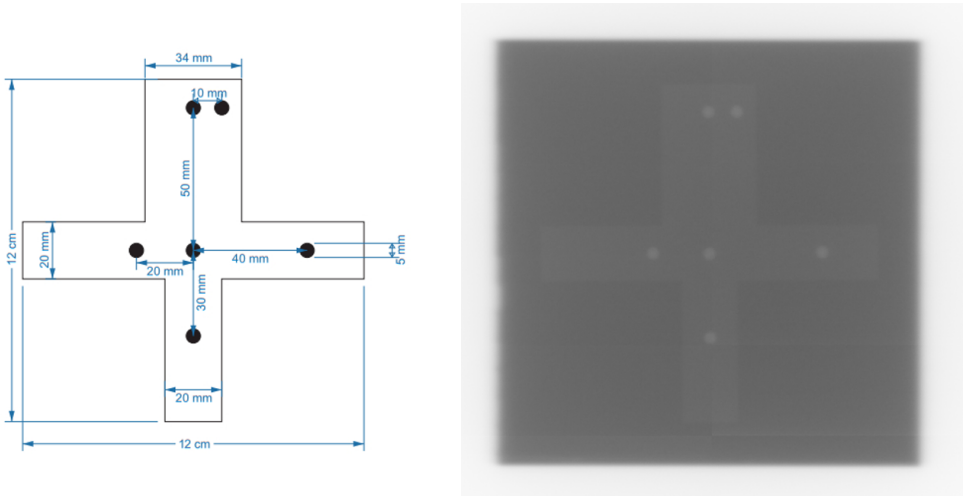

Figure 5: Scaling phantom and its image, developed for calibrating distances and thickness in developed softwire.

software developed in this study are presented in Table 1. To establish the EPID limitations for distinguishing lines and accurately determining the size of each line from the provided radiation image as depicted in the Fig. 6, four distances between the lines have been considered: 1, 1.5, 2, and 2.5 mm.

Table 2: Scaling parameter for centers A and B, for different widths of the lines and distances between the lines .

	Scaling (pixel per mm)							
	Distances between the lines (mm)							
	1		1.5		2		2.5	
Line width (mm)	A	B	A	B	A	B	A	B
2	1.91	1.90	2.01	2.1	2.01	1.9	2.01	2.01
1.5	1.4	1.35	1.51	1.7	1.51	1.5	1.5	1.5
1	0.8	0.80	1.10	1.2	1.00	0.9	1.0	1.0

The widths of the lines are 2, 1.5, and 1 mm, respectively. The analysis results were obtained using software developed specifically for this study. Increased line spacing enhances the EPID's capability to differentiate lines, leading to a more precise measurement of each line's width. It is essential to measure most quality control parameters at the time of EPID initialization and to assess the variations against the baseline values. The results, shown in Table 2, indicate the EPID's ability to resolve line spacings and widths accurately. For Center A, scaling values ranged from 0.8 to 2.01 pixels/mm, and for Center B, from 0.8 to 2.1 pixels/mm, across different line widths and spacings. Increased line spacing improved line differentiation, enhancing measurement precision. Both centers achieved resolution exceeding the TG142 standard of 2 mm.

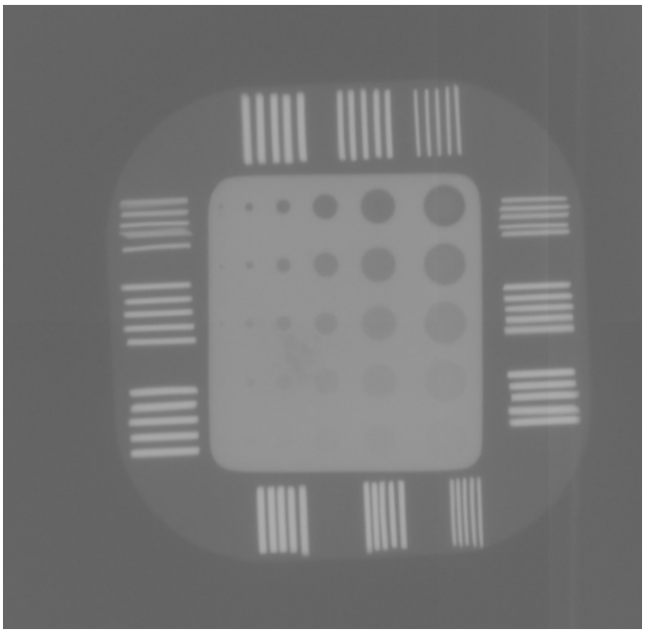

Figure 6: An image of developed phantom.

4 Conclusions

The development and implementation of a quality control phantom for electronic portal imaging devices (EPIDs) have proven to be effective in ensuring consistent image quality and stable radiation response in radiation therapy. The designed phantom, utilizing lead sheets of varying thicknesses and a plexiglass scaling component, facilitated comprehensive evaluation of critical image quality parameters, including Noise, Uniformity, Contrast-to-Noise Ratio (CNR), Signal-to-Noise Ratio (SNR), Contrast, and pixel-to-millimeter scaling. The accompanying LabVIEW-based software streamlined the analysis process, providing standardized and automated assessments of EPID performance across two radiotherapy centers. Results demonstrated variations in image quality factors between the centers, with Center A showing lower Noise (0.5 vs. 1.6) and Uniformity (1.9 vs. 9.3) and higher CNR (69.3 vs. 45.6) and SNR values compared to Center B, indicating differences in EPID performance. The phantoms design, inspired by established models like the Las Vegas and PTW phantoms, allowed for both qualitative and quantitative evaluations, meeting the TG142 standard for spatial resolution (> 2 mm). This study underscores the importance of tailored quality assurance tools and software in enhancing the precision and reliability of EPID systems, ultimately contributing to improved accuracy in radiation therapy delivery and patient outcomes. Future work could focus on expanding the phantoms application to other EPID models and integrating additional quality control parameters to further refine radiotherapy imaging protocols.

Conflict of Interest

The authors declare no potential conflict of interest regarding the publication of this work.

Funding

The authors declare that no funds, grants, or other financial support were received during the preparation of this manuscript.

References

Association, N. E. M. et al. (2004). National Electrical Manufacturers Association. *Digital Imaging and Communications in Medicine (DICOM)*.

Boudet, J., Aubignac, L., Beneux, A., et al. (2022). Evaluation of QA software system analysis for the static picket fence test. *Journal of Applied Clinical Medical Physics*, 23(7):e13618.

Cho, J.-H., Lee, J.-H., Jung, J.-Y., et al. (2015). Evaluation of image quality for various electronic portal imaging devices in

radiation therapy. *Journal of Radiological Science and Technology*, 38(4):451–461.

Cremers, F., Frenzel, T., Kausch, C., et al. (2004). Performance of electronic portal imaging devices (EPIDs) used in radiotherapy: image quality and dose measurements. *Medical Physics*, 31(5):985–996.

Diklic, A., Dundara Debeljuh, D., Jurkovic, S., et al. (2013). Quality Control of Mega Voltage Portal Imaging System.

Dogan, N., Mijnheer, B. J., Padgett, K., et al. (2023). AAPM Task Group Report 307: use of EPIDs for patient-specific IMRT and VMAT QA. *Medical Physics*, 50(8):e865–e903.

El-Bassiouni, M., Davis, J. B., El-Attar, I., et al. (2006). Target motion variability and on-line positioning accuracy during external-beam radiation therapy of prostate cancer with an endorectal balloon device. *Strahlentherapie und Onkologie*, 182(9):531–536.

Gagel, B., Schramm, O., Harms, W., et al. (2002). The Electronic Portal Imaging System Siemens Beamview Plus® Versus the Conventional Verification Films CEA-TVS® and DuPont CQL-7® A Critical Appraisal of Visual Image Quality: A Critical Appraisal of Visual Image Quality. *Strahlentherapie und Onkologie*, 178(8):446–452.

Herman, M. G., Balter, J. M., Jaffray, D. A., et al. (2001). Clinical use of electronic portal imaging: report of AAPM Radiation Therapy Committee Task Group 58. *Medical Physics*, 28(5):712–737.

Huang, M., Huang, D., Zhang, J., et al. (2017). Preliminary study of clinical application on IMRT three-dimensional dose verification-based EPID system. *Journal of Applied Clinical Medical Physics*, 18(4):97–105.

Klein, E. E., Hanley, J., Bayouth, J., et al. (2009a). Quality assurance of medical accelerators: report of AAPM Radiation Therapy Committee Task Group 142. *Medical Physics*, 36:4197–4212.

Klein, E. E., Hanley, J., Bayouth, J., et al. (2009b). Task Group 142 report: Quality assurance of medical accelerators. *Medical Physics*, 36(9Part1):4197–4212.

Kruse, J. J., Herman, M. G., Hagness, C. R., et al. (2002). Electronic and film portal images: a comparison of landmark visibility and review accuracy. *International Journal of Radiation Oncology* Biology* Physics*, 54(2):584–591.

Kry, S. F., Bednarz, B., Howell, R. M., et al. (2017). AAPM TG 158: measurement and calculation of doses outside the treated volume from external-beam radiation therapy. *Medical Physics*, 44(10):e391–e429.

Lee, S., Yan, G., Bassett, P., et al. (2016). Use of local noise power spectrum and wavelet analysis in quantitative image quality assurance for EPIDs. *Medical Physics*, 43(9):4996–5008.

Li, Y., Chen, L., Zhu, J., et al. (2017). A quantitative method to the analysis of MLC leaf position and speed based on EPID and EBT 3 film for dynamic IMRT treatment with different types of MLC. *Journal of Applied Clinical Medical Physics*, 18(4):106–115.

McGarry, C., Grattan, M., and Cosgrove, V. (2007). Optimization of image quality and dose for Varian aS500 electronic portal imaging devices (EPIDs). *Physics in Medicine & Biology*, 52(23):6865.

Noble, D., Ramaesh, R., Brothwell, M., et al. (2024). The evolving role of novel imaging techniques for radiotherapy planning. *Clinical Oncology*, 36(8):514–526.

Peca, S., Sinha, R. S., Brown, D. W., et al. (2017). In vivo portal imaging dosimetry identifies delivery errors in rectal cancer radiotherapy on the belly board device. *Technology in Cancer Research & Treatment*, 16(6):956–963.

Tzomakas, M. K., Peppa, V., Alexiou, A., et al. (2023). A phantom based evaluation of the clinical imaging performance of electronic portal imaging devices. *Heliyon*, 9(10).

©2025 by the journal.

RPE is licensed under a Creative Commons Attribution-NonCommercial 4.0 International License (CC BY-NC 4.0).

To cite this article:

Hajiloo, N. , Mohammadi, M. , Ghasemifard, F. and Aghamiri, M. (2025). Design and construction of a quality control phantom for evaluation of the clinical imaging performance of electronic portal imaging devices. *Radiation Physics and Engineering*, 6(4): 39-45. doi: 10.22034/rpe.2025.528889.1279

DOI: 10.22034/rpe.2025.528889.1279

To link to this article: https://doi.org/10.22034/rpe.2025.528889.1279